Electron-concentration and pressure-induced structural changes in the alloys $In_{1-x}X_x$ (X=Cd,Sn)

A. S. Mikhaylushkin,[1,2] S. I. Simak,[2,3] B. Johansson,[2,4] and U. Häussermann[1]
[1]*Department of Inorganic Chemistry, Stockholm University, S-106 91 Stockholm, Sweden*
[2]*Department of Physics, Uppsala University, Box 530, SE-751 21 Uppsala, Sweden*
[3]*Theory and Modeling, IFM, Linköping University, S-581 83, Linköping, Sweden*
[4]*Applied Materials Physics, Department of Materials and Engineering, Royal Institute of Technology (KTH), SE-10044 Stockholm, Sweden*
(Received 20 January 2005; revised manuscript received 5 July 2005; published 19 October 2005)

Electron-concentration and pressure-induced structural transitions in solid solutions $In_{1-x}Cd_x$ ($0 \leqslant x \leqslant 0.1$) and $In_{1-x}Sn_x$ ($0 \leqslant x \leqslant 0.2$) have been investigated by means of first principles calculations. At ambient pressure the structural sequence face-centered cubic → body-centered tetragonal ($c/a > \sqrt{2}$) → body-centered tetragonal ($c/a < \sqrt{2}$) is realized with increasing of valence electron concentration (VEC). High pressure has the same effect as the increase of electron concentration shifting the occurrence of the structural transitions to lower-valence electron concentration. The driving force behind the peculiar structural sequence is an enhancement of *s-p* hybridization with increasing VEC.

DOI: 10.1103/PhysRevB.72.134202 PACS number(s): 61.66.Dk

I. INTRODUCTION

Elemental indium adopts a simple but unique crystal structure deviating from the close-packed trend usually displayed by metallic elements. It features a body-centered tetragonal (bct) unit cell that contains two equivalent atoms at the corners and at the center. The lattice parameters (at room temperature) are $a=3.2522$ Å and $c=4.9507$ Å.[1] As a consequence, bct-In corresponds to a slightly distorted face-centered cubic (fcc) structure with a c/a ratio of 1.522, compared to $c/a=\sqrt{2}$ for ideal fcc. The environment of the 12 nearest neighbors in the fcc structure is split into two sets of four (at the distance $d=3.252$ Å) and eight ($d=3.379$ Å) atoms, respectively. Alternatively, the In structure can be looked upon as face-centered tetragonal (fct) with $(c/a)_{fct}=1.076$.[2]

The origin of the bct structure of In is not immediately clear. The lighter homologue Al crystallizes in the fcc structure. On the grounds of pseudopotential theory Heine and Weaire[3] and later Hafner and Heine[4] argued that the larger ionic core of In compared to Al drives an instability of the fcc structure. More recently we demonstrated from first-principles calculations that the stabilization which In gains by distortion of the fcc structure is only about 1–2 meV per atom.[5] Remarkably this small energy difference persists up to very high pressures,[6] although one could have expected that the tetragonal distortion is easily removed by application of external pressure. Available high-pressure experiments confirm the stability of the bct structure.[7–9] Thus only under extreme compression the bct-In is predicted to undergo that transition into the fcc structure at pressure of about 800 GPa.[6] It was found that the tetragonal distortion in In actually is connected with an increase of *s-p* hybridization of the valence bands.[5,6] This hybridization parallels the band energy part of the total energy and drives the structural stability for the group III A elements.[10,11] For Al the *s-p* hybridization is optimized in the fcc ground state structure, whereas for In the *s-p* hybridization increases with increasing tetragonal distortion.

In this light, solid solutions $In_{1-x}Cd_x$ and $In_{1-x}Sn_x$ demonstrate a remarkable structural sequence. To a first approximation the alloying leads to a decrease (for Cd) and increase (for Sn) of the valence electron concentration. A 4–5 at. % alloying with Cd results in a discontinuous change to the fcc structure.[1,12,13] The solubility of Cd in the fcc phase is around 20 at. %.[14] In contrast to this, alloying with Sn increases first the bct c/a axial ratio.[15] At 12–14 at. % Sn a structural change to a bct structure with $c/a < \sqrt{2}$ occurs (the so-called β-phase).[16] In the following we denote this structure as bct-II and the bct-In structure with $c/a > \sqrt{2}$ as bct-I. Under pressure the alloy $In_{0.80}Sn_{0.20}$ remains in the bct-II structure up to at least 30 GPa.[17] Again, $In_{0.94}Cd_{0.06}$ transforms at 1.4 GPa from the fcc into the bct-I structure.[17] The latter structure is stable up to at least 30 GPa.

Indium is situated at the borderline between metals and nonmetals in the Periodic Table and apparently its elemental bct-I structure is most sensitive to changes in the electron concentration. In the present work we have investigated the electronic structure of the solid solutions $In_{1-x}Cd_x$ ($0 \leqslant x \leqslant 0.1$) and $In_{1-x}Sn_x$ ($0 \leqslant x \leqslant 0.2$) by means of first-principles calculations. We analyze electron concentration and pressure effects on structural competition between the bct-I, bct-II, and fcc structures in In-rich solid solution. We argue that the tetragonal distortion of the fcc structure leads to an increase of hybridization of the 5*s* and 5*p* valence bands and, consequently, a gain of the band energy. On the other hand the electrostatic contribution to the total energy has a minimum for the fcc structure. Hence, the subtle c/a-ratio variations in the considered alloys appear as a consequence of these two counteracting trends.

II. COMPUTATIONAL DETAILS

Total energy calculations were performed in the framework of the frozen core all-electron projected augmented wave (PAW) method[18,19] as implemented in the program VASP.[20,21] $In_{1-x}Sn_x$ and $In_{1-x}Cd_x$ solid solutions were de-

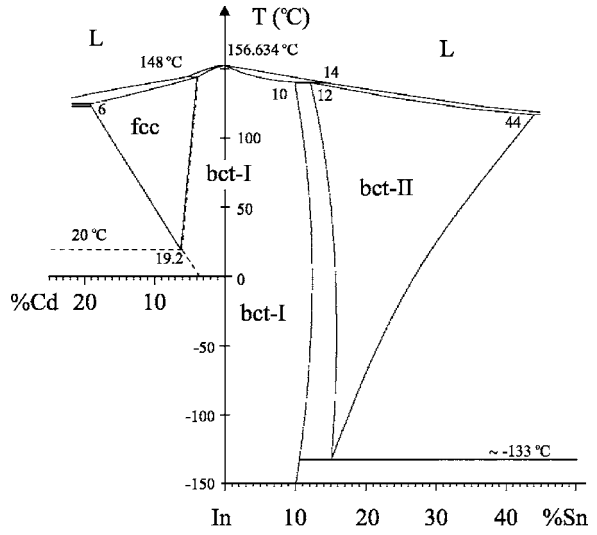

FIG. 1. In-rich parts of the phase diagrams $In_{1-x}Cd_x$ and $In_{1-x}Sn_x$ according to Massalski (Ref. 14).

scribed by the virtual crystal approximation (VCA). This assumes that electrons in an alloy behave identically to the electrons in hypothetical ordered material in which the charge density of the crystalline potential is the average of the charges densities of the pure materials. It is clear that the subtle interplay between different atoms is lost in this approximation. However, since Cd and Sn are situated next to In in the Periodic Table, such approximation is expected to be reliable.[22] For that we used the In pseudopotential parameters with total nuclear and electron charge that corresponded to the average total charge in the modeled solid solutions. The energy cutoff was set to 500 eV. Exchange and correlation effects were treated by the generalized gradient approximation (GGA).[23] The integration over the Brillouin zone (BZ) was done with the linear tetrahedron method with Blöchl corrections[24] using a grid of special k points determined according to the Monkhorst-Pack scheme.[25] 3078 irreducible k points in the bct BZ were taken into account. For band structure calculations the integration was done according to Methfessel-Paxton[26] using a fine grid of special k points. All necessary convergency tests were performed and total energies were converged to at least 0.1 meV/atom. It should be mentioned that the pressure dependence of the volumes of all considered bct structural arrangements of $In_{1-x}Cd_x$ and $In_{1-x}Sn_x$ is virtually indistinguishable from that of bct-I In.

III. RESULTS

A. Ambient pressure concentration structural sequence

The In-rich parts of the zero pressure phase diagrams of $In_{1-x}Cd_x$ and $In_{1-x}Sn_x$ are assembled in Fig. 1.[14] On the Cd side, the phase boundary between the bct-I and fcc phases corresponds to a straight line between the temperatures 20 °C and 148 °C and the concentrations $x_{Cd}=0.06$ and $x_{Cd}=0.04$. The fcc phase obtains a maximum solubility $x_{Cd}=0.19$ around 127 °C. On the Sn side, the bct-I In structure is stable until concentrations around $x_{Sn}=0.10-0.11$. There is a small two-phase region from $x_{Sn}\approx 0.11$ to ≈ 0.13 between −133 °C and 140 °C. For higher concentrations x_{Sn} the bct-II phase occurs, which is stable until −133 °C, and extends to $x_{Sn}=0.44$ at 120 °C.

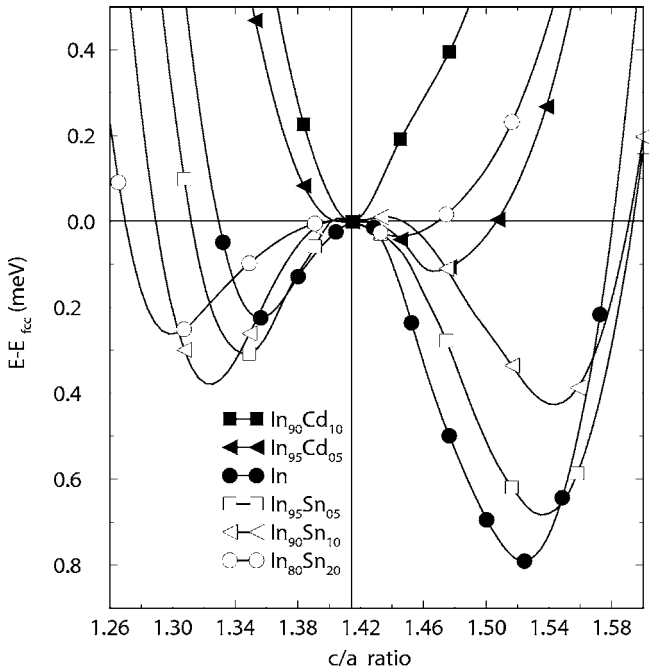

FIG. 2. Variation of $E-E_{fcc}$ as a function of c/a for $In_{1-x}Cd_x$ ($x=0.10, 0.05$), In, and $In_{1-x}Sn_x$ ($x=0.10, 0.20$) at the respective ground-state volumes.

Figure 2 presents the total energy per atom (at zero temperature) as a function of the bct c/a ratio for different concentrations x_{Cd} and x_{Sn}. Most of the curves display a characteristic double-well behavior. Two minima corresponding to the bct-I and bct-II structures are separated by a local maximum at $c/a=\sqrt{2}$, which is the fcc structure. The energy differences between the three structural arrangements are extremely small. For In the bct-I structure is stabilized over the bct-II and fcc structure by just 0.6 and 0.8 meV/atom, respectively. The c/a ratio of bct-I is 1.52, which is in excellent agreement with the experimental value. For $In_{0.95}Cd_{0.05}$ the differences become virtually zero and for $In_{0.90}Cd_{0.10}$ the total energy minimum is located at $c/a=\sqrt{2}$, i.e., the fcc structure is most stable. This coincides with the room temperature structural change in $In_{1-x}Cd_x$ occurring around $x=0.06$. For $In_{0.90}Sn_{0.10}$ the minima for the bct-I and bct-II structures have about the same depth. For $In_{0.80}Sn_{0.20}$ the bct-II structure with a $c/a\approx 1.30$ is most stable. Again, this coincides with the experimental room temperature situation: For $In_{1-x}Sn_x$ the composition $x=0.10$ is close to the two-phase region bct-I/bct-II and the experimental c/a ratio for bct-II $In_{0.80}Sn_{0.20}$ is 1.283.[27] The calculated variations of c/a and volume as a function of electron concentration VEC in the range between 2.9 e/at. ($In_{0.90}Cd_{0.10}$) and 3.2 e/at. ($In_{0.80}Sn_{0.20}$) are shown in Fig. 3, together with the experimental values where available. The structural transitions are not accompanied with a change in volume. The good agreement between theoretical and experimental data justifies the applied VCA approximation for describing the solid solutions $In_{1-x}Cd_x$ and $In_{1-x}Sn_x$.

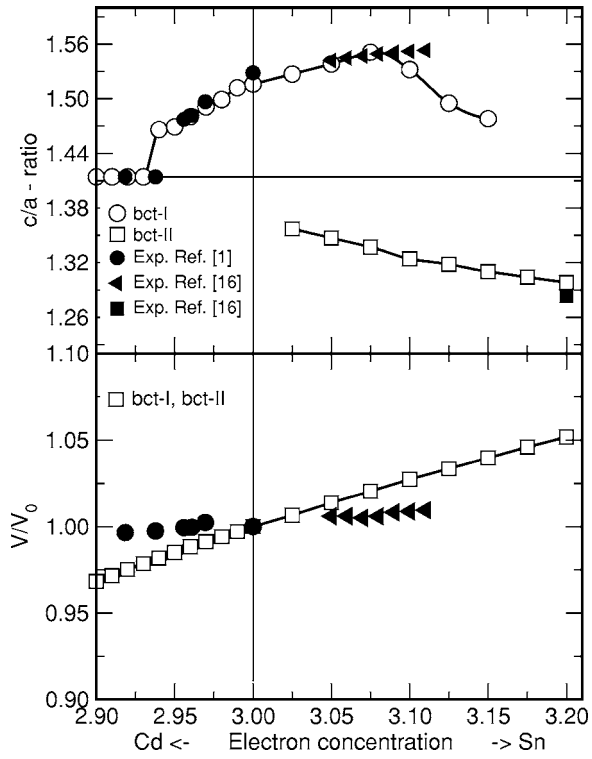

FIG. 3. Variation of the c/a ratio and the equilibrium volume in alloys $In_{1-x}Cd_x$ and $In_{1-x}Sn_x$ for a range of VEC between 2.9 and 3.2 e/at. Experimental values are indicated by open symbols.

B. Pressure-induced phase transformations

The double-well behavior of the total energy upon the tetragonal c/a variation as shown in Fig. 2 is remarkable. The energy differences between the fcc and bct structures are extremely low and are exceeded by far by the thermal energy at room temperature. Recently we could show that the bct-II minimum in elemental In actually is not stable with respect to an orthorhombic distortion of the lattice and represents a saddle point in the energy contour $E(c/a,b/a)$.[28]

In Fig. 4 we assembled contours $E(c/a,b/a)$ for $In_{0.90}Cd_{0.10}$, $In_{0.95}Cd_{0.05}$, In, $In_{0.95}Sn_{0.05}$, and $In_{0.90}Sn_{0.10}$ at ambient and elevated pressure. Now we choose to describe the structure of In as fct rather than bct. The bct-I (bct-II) structure has the axial ratios $b/a_{fct}=1$, $c/a_{fct}>1$ ($b/a_{fct}=c/a_{fct}>1$). The c/a_{fct} and b/a_{fct} ratios were varied in the range from 1 to 1.2. At zero pressure with decreasing VEC (increasing x_{Cd}) the two minima corresponding to bct-I start merging and the fcc structure becomes most stable. With increasing VEC (increasing x_{Sn}) these two minima become smeared out towards the bct-II structure, which becomes a local minimum for VEC=3.1. The situation for VEC=3.1 with two different, but hardly separated, local minima (bct-I and bct-II) represents a peculiar situation. According to the In—Sn phase diagram (cf. Fig. 1) the composition $x_{Sn}=0.10$ is close to the two-phase region consisting of an In-richer bct-I and a Sn-richer bct-II phase. With pressure In enters this peculiar situation at about 48 GPa. However, In is a one-component system and cannot have an extended thermodynamically stable two-phase region with pressure variation at a given temperature (here, 0 K). The situation can be explained by assuming a rapid dynamical fluctuation between bct-I and bct-II with a face-centered orthorhombic (fco) transition state as the separating saddle point. This saddle point represents an extremely tiny barrier and the bct-I $\rightleftharpoons$ bct-II fluctuations in high-pressure In were suggested.[28] As a consequence the experimentally observed structure under pressure is the (smeared) out transition (fco) state. This interpretation matches the experimentally determined structure of In-II between 45 and 90 GPa.[8]

$In_{1-x}Cd_x$ with the fcc structure transforms into the bct-I structure under pressure. This is in agreement with the experimental finding. Degtyareva *et al.* obtained a transition pressure of 1.4 GPa for $In_{0.94}Cd_{0.06}$,[17] which has a composition close to the homogeneity range border. For $In_{0.90}Cd_{0.10}$ we calculate a fcc $\rightarrow$ bct-I transition pressure of 37 GPa. $In_{0.96}Sn_{0.04}$ with the bct-I structure has been the subject of an experimental high-pressure investigation.[29] No transition was observed until 20 GPa. According to our 0 K calculations $In_{1-x}Sn_x$ solid solutions with the bct-I structure ($x\leqslant 0.10$) transform to the bct-II structure under pressure. $In_{0.95}Sn_{0.05}$ enters a situation at 30 GPa which corresponds to that of In at higher pressures or $In_{0.90}Sn_{0.10}$ at ambient conditions. Thus, a phase separation into an In-richer bct-I and a Sn-richer bct-II phase should occur. Such a behavior was observed for the In-Pb alloy $In_{0.90}Pb_{0.10}$.[30] For $In_{0.90}Sn_{0.10}$ the ambient condition two-minima contour (two-phase situation) disappears rapidly with pressure. Above 5 GPa only the minimum corresponding to the bct-II structure is present. $In_{0.80}Sn_{0.20}$ adopts the bct-II structure already at ambient conditions. Experimentally this structure is maintained until 30 GPa[17] and according to our calculations even up to at least 400 GPa.

The high-pressure behavior of $In_{1-x}Cd_x$ and $In_{1-x}Sn_x$ alloys spanning a range of VEC from 2.9 to 3.2 e/at. is summarized in Fig. 5. It is immediately apparent that high pressure has the same effect as the increase of VEC. Alloys $In_{1-x}Cd_x$ with the fcc structure transform to the bct-I structure found for VEC between 2.95 and 3.10 at zero pressure. In and $In_{0.95}Sn_{0.05}$ with the bct-I structure transform to a two-minima (two-phase region) situation found for VEC between 3.10 and 3.14 at zero pressure. Alloys $In_{1-x}Sn_x$ with a composition close to the two-phase region transform to the bct-II structure found for VEC >3.14 at zero pressure. Once the bct-II structure is obtained (either compositionally or under pressure) it remains stable under high pressures.

IV. DISCUSSION

With increasing VEC from 2.9 to 3.2, In alloys display the structural sequence fcc $\rightarrow$ bct-I $\rightarrow$ bct-II. To elaborate on the nature of this sequence we consider the electronic structure of elemental In. Its density of state (DOS) is depicted in Fig. 6. At low energies the DOS shows a parabolic, free-electronlike distribution, which is succeeded by a sequence of three pronounced wells at higher energy. It is noticeable that the $5s$ and $5p$ bands are rather separated. The Fermi level is exactly located at the third well for $c/a>\sqrt{2}$ (bct-I), but slightly displaced for $c/a=\sqrt{2}$ (fcc) and $c/a<\sqrt{2}$ (bct-II).

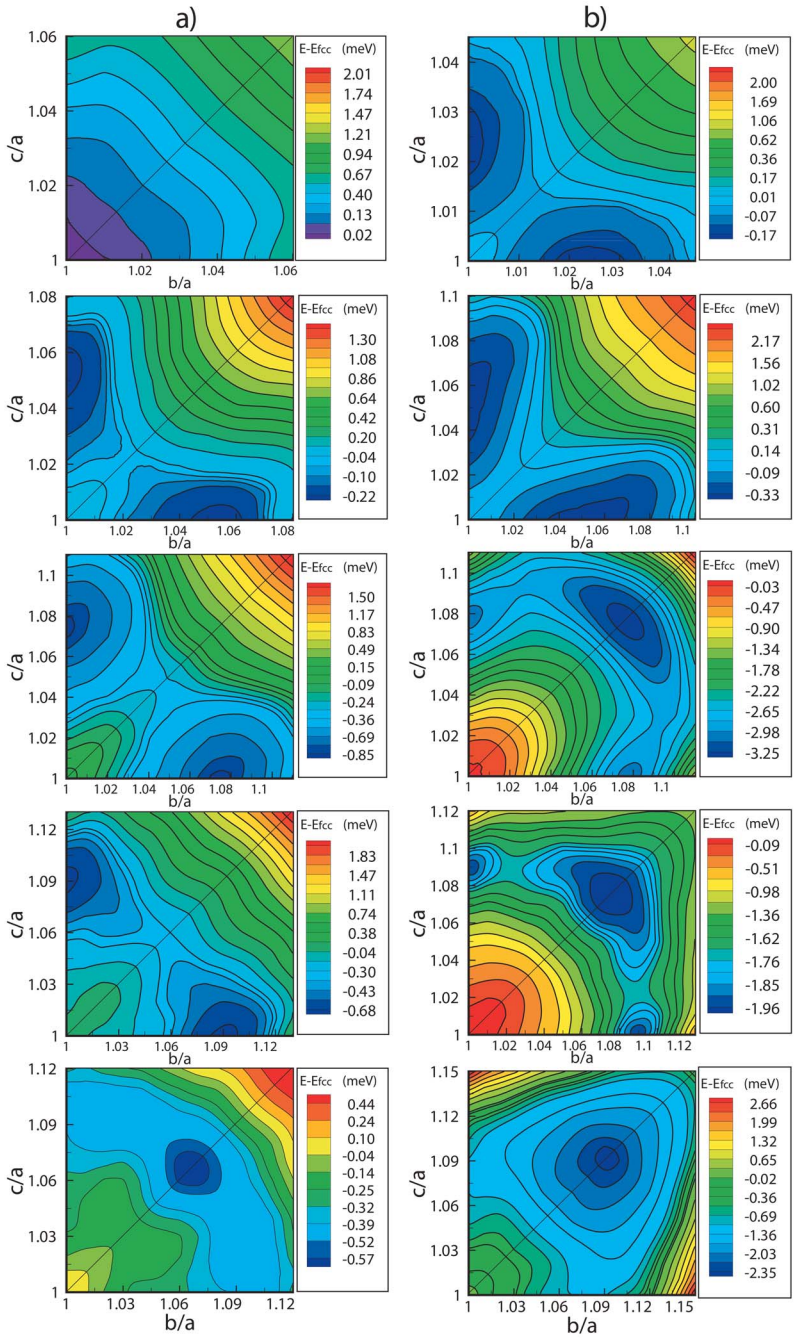

FIG. 4. (Color online) Total energy difference $E-E_{fcc}$ of $In_{0.90}Cd_{0.10}$, $In_{0.95}Cd_{0.05}$, In, $In_{0.95}Sn_{0.05}$, $In_{0.90}Sn_{0.10}$ at ambient conditions (a) and $In_{0.90}Cd_{0.10}$ at 37 GPa, $In_{0.95}Cd_{0.05}$ at 30 GPa, In at 85 GPa, and $In_{0.95}Sn_{0.05}$ at 30 GPa (b).

For small concentrations of Cd and Sn the electronic structure of the alloys follow a rigid band behavior with respect to In. Fig. 7 shows the value of the DOS at the Fermi level, DOS(E_F), for bct-I, bct-II, and fcc as a function of the electron concentration. The stability ranges of the different phases are surprisingly well reproduced when considering the structure with the lowest value of DOS(E_F) at each VEC. Thus, In-Cd and In-Sn alloys adopt the structure in which the Fermi level is adjusted as close as possible to the local minimum of the DOS. Importantly, as seen in Fig. 6, the depth and the exact location of this well is influenced by the tetragonal c/a variation. As shown recently, this is due to subtle changes in the degree of hybridization of the 5*s* and 5*p* valence bands.[5,6] Indium, and generally all group III A elements, adopt a structure in which an optimum situation of *s-p* hybridization and electrostatic energy can be realized.[10,11] The considered In alloys with VEC between 2.9 and 3.2 appear to follow the same structural stability principle.

Changes in the hybridization of 5*s* and 5*p* valence bands are, of course, reflected in the band energy part of the total energy. Enhancement of *s-p* hybridization upon increasing the tetragonal distortion in pure In at ambient pressure results in a lowering of the band energy. Contrary, the electrostatic energy has a minimum for the undistorted fcc structure. Hence, the simultaneous minimization of two counteracting trends provides a certain c/a ratio for pure In. In the next step we investigate the effect of alloying on the band energy.

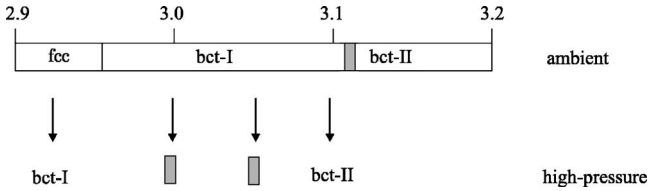

FIG. 5. Schematic summary of the ambient condition and high-pressure structures occurring in $In_{1-x}Cd_x$ and $In_{1-x}Sn_x$ for a range of VEC between 2.9 and 3.2 e/at. Two-phase regions are indicated as the gray areas.

Figure 8 depicts the band energy of the fcc and total-energy minimized bct-I and bct-II structures as a function of VEC. At ambient pressure pure In (VEC=3) attains the lowest band energy in the bct-I structure. Alloying In with Cd (VEC$<$3) decreases the band energy difference between the fcc and the two bct structures. At about 7 at. % Cd the phase transition bct-I $\rightarrow$ fcc takes place. When In is alloyed with Sn (VEC$>$3) the band energy of the bct-I phase decreases first and becomes a minimum at about 8 at. % of Sn. Upon a further increase of VEC the bct-I band energy increases again with respect to the band energies of the fcc and bct-II structures. Contrary, the bct-II band energy decreases monotonically over the whole range of considered VEC. At

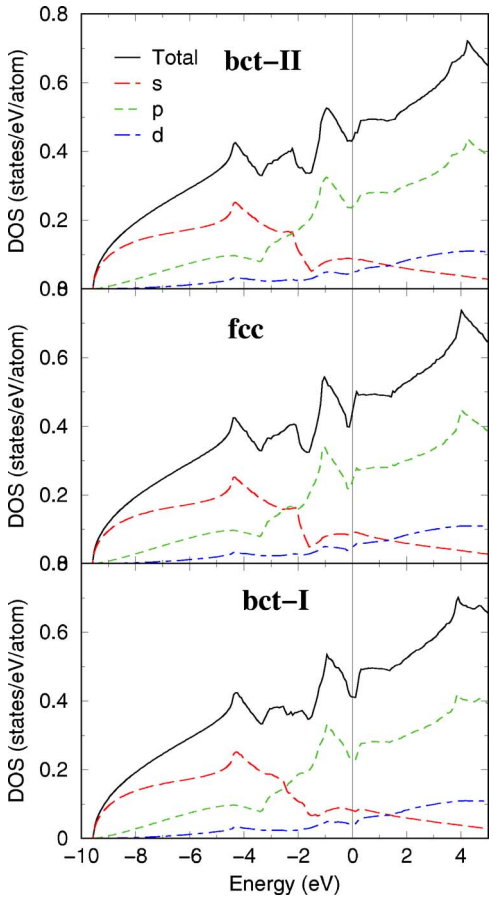

FIG. 6. (Color online) Total DOS together with the s, p, and d orbital contributions for In in the bct-II, fcc, and bct-I structure at the ground-state volume.

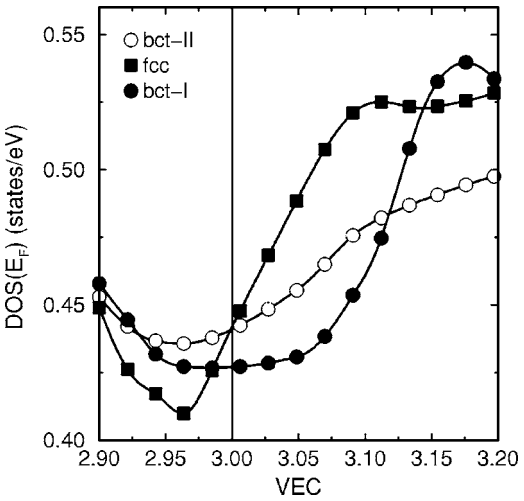

FIG. 7. Value of the DOS at the Fermi level [DOS(E_F)] for $In_{1-x}X_x$ ($2.9 \leqslant \mathrm{VEC} \leqslant 3.2$ e/at.) in the bct-II, fcc, and bct-I structure.

$\approx$13 at. % Sn the band energy of bct-II has become lower than that of bct-I, which agrees with the two-phase region bct-I and bct-II, and finally the stability of the bct-II phase at even higher Sn concentrations. Pressure increases considerably the band energy differences between the fcc and the two bct structures, which coincides with the increased range of existence of the bct-I phase in alloys $In_{1-x}Cd_x$. Also, with pressure the band energy difference between the two bct structures diminishes, which coincides with the increased stability range of the bct-II phase towards lower VEC in alloys $In_{1-x}Sn_x$. Thus the trends in the band energy parallel

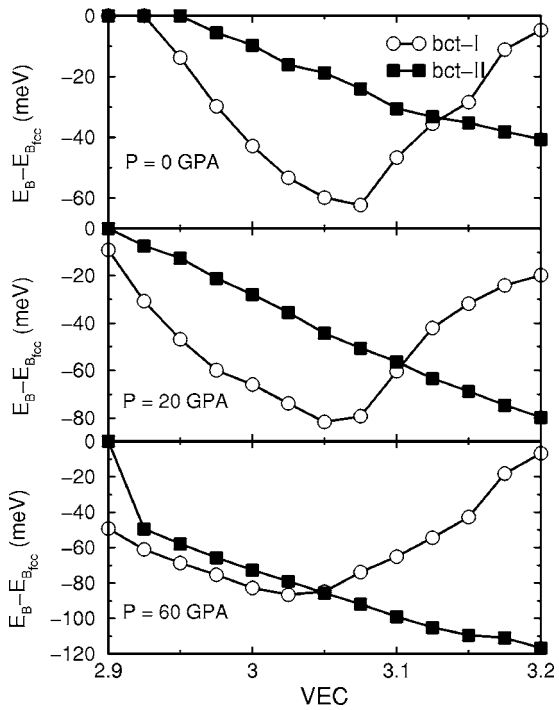

FIG. 8. The band energy of the bct-I and bct-II structures with respect to fcc as a function of VEC at (a) ambient conditions, (b) 20 GPa, and (c) 60 GPa.

nicely the structural sequence fcc → bct-I → bct-II found for In-Cd and In-Sn alloys with increasing VEC at ambient conditions and high pressure.

The clear correlation between VEC and the different structures occurring in In alloys has prompted Degtyareva *et al.* to apply simple free-electronlike Fermi surface-Brillouin zone interactions for a possible interpretation.[17,30,31] This argumentation is hampered somewhat from the fact that the Fermi surface of In alloys cannot be considered as an electron sphere as it is for Cu-based Hume-Rosery phases.[32] However, the structural stability in In alloys can be understood with the effect of *s-p* mixing of the valence bands.[5,6,10] This mixing releases partly *s-s* antibonding states above the Fermi level which in the unhybridized (free-electronlike) case would have been occupied for a considerable part of the Brillouin zone. A consequence of *s-p* mixing of the valence bands is the appearance of local band gaps at high-symmetry points, which are reflected in the DOS as wells. For In and its Cd and Sn alloys it is favorable to attain a structure in which *s-p* mixing is optimized and thus the Fermi level located as close as possible to a well in the DOS (cf. Fig. 7).

V. CONCLUSIONS

We investigated electron-concentration and pressure-induced structural transitions in alloys $In_{1-x}Cd_x$ ($0 \leqslant x \leqslant 0.1$) and $In_{1-x}Sn_x$ ($0 \leqslant x \leqslant 0.2$) by means of first principles calculations. At ambient conditions the structural sequence fcc → bct-I → bct-II is realized with increasing VEC. The stability ranges of the different phases are very well reproduced when considering the structure producing the lowest value of DOS(E_F) at a particular VEC as most stable. At the transition bct-I → bct-II a two-phase region is encountered. In our calculations this is reflected by two very close-lying local minima on the energy contour $E(c/a, b/a)$. High pressure has the same effect as the increase of VEC. Alloys $In_{1-x}Cd_x$ with the fcc structure transform to bct-I and alloys $In_{1-x}Sn_x$ with the bct-I structure transform to a two-phase region or pure bct-II, depending on their composition. Elemental In represents a peculiar case.[28] According to our total energy calculations, In also reveals a pressure-induced transition from its bct-I ground state to a two-phase mixture. This, however, cannot be realized by a one-component system over an extended range of pressure. Instead, a rapid, dynamical, fluctuation between bct-I and bct-II in respectively large domains of the bct-In matrix is assumed with a face-centered orthorhombic (fco) transition state as the separating saddle point.

ACKNOWLEDGMENTS

This work was supported by the Swedish National Science Foundation (VR) and the Swedish Foundation for Strategic Research (SSF). Calculations were partly done at the National Supercomputer Center (NSC) in Linköping, Sweden. Further, we acknowledge highly stimulating discussions with V. F. Degtyareva.

[1] M. E. Straumanis, P. B. Rao, and W. J. James, Z. Metallkd. **62**, 493 (1971).
[2] P. Villars and L. D. Calvert, *Pearson's Handbook of Crystallographic Data for Intermetallic Phases* (American Society for Metals, Metals Park, Ohio, 1985).
[3] V. Heine and D. Weaire, Solid State Phys. **24**, 249 (1970).
[4] J. Hafner and V. Heine, J. Phys. F: Met. Phys. **13**, 2479 (1983).
[5] U. Häussermann, S. I. Simak, R. Ahuja, B. Johansson, and S. Lidin, Angew. Chem., Int. Ed. Engl. **38**, 2017 (1999).
[6] S. I. Simak, U. Häussermann, R. Ahuja, S. Lidin, and B. Johansson, Phys. Rev. Lett. **85**, 142 (2000).
[7] K. Takemura, Phys. Rev. B **44**, 545 (1991).
[8] K. Takemura and H. Fujihisa, Phys. Rev. B **47**, 8465 (1993).
[9] O. Schulte and W. B. Holzapfel, Phys. Rev. B **48**, 767 (1993).
[10] U. Häussermann, S. I. Simak, R. Ahuja, and B. Johansson, Angew. Chem., Int. Ed. Engl. **39**, 1246 (2000).
[11] U. Häussermann, S. I. Simak, R. Ahuja, and B. Johansson, Phys. Rev. Lett. **90**, 065701 (2003).
[12] T. Heumann and B. Predel, Z. Metallkd. **50**, 309 (1959).
[13] T. Heumann and B. Predel, Z. Metallkd. **53**, 240 (1962).
[14] T. B. Massalski, H. Okamoto, P. R. Subramanian, and L. Kacprzak, *Binary Alloys Phase Diagrams* (ASM International, Materials Park, Ohio, 1990) Vol. 3.
[15] M. F. Merriam, Phys. Rev. Lett. **11**, 321 (1963).
[16] T. Heumann and O. Alpaut, J. Less-Common Met. **6**, 108 (1964).
[17] O. Degtyareva, V. F. Degtyareva, F. Porsch, and W. Holzapfel, J. Phys.: Condens. Matter **13**, 7295 (2001).
[18] P. E. Blöchl, Phys. Rev. B **50**, 17953 (1994).
[19] G. Kresse and D. Joubert, Phys. Rev. B **59**, 1758 (1999).
[20] G. Kresse and J. Hafner, Phys. Rev. B **48**, 13115 (1993).
[21] G. Kresse and J. Furthmüller, Cell Motil. Cytoskeleton **6**, 15 (1996).
[22] L. Nordheim, Ann. Phys. **9**, 607 (1931); L. Bellaiche and D. Vanderbilt, Phys. Rev. B **61**, 7877 (2000); S. de Gironcoli, P. Giannozzi, and S. Baroni, Phys. Rev. Lett. **66**, 2116 (1991); A. M. Saitta, S. de Gironcoli, and S. Baroni, *ibid.* **80**, 4939 (1998); D. A. Papaconstantopoulos and W. E. Pickett, Phys. Rev. B **57**, 12751 (1998); L. Bellaiche, S.-H. Wei, and A. Zunger, Appl. Phys. Lett. **70**, 3558 (1997); U. Häussermann, S. I. Simak, I. A. Abrikosov, B. Johansson, and S. Lidin, J. Am. Chem. Soc. **120**, 10136 (1998).
[23] Y. Wang and J. P. Perdew, Phys. Rev. B **44**, 13298 (1991); J. P. Perdew, J. A. Chevary, S. H. Vosko, K. A. Jackson, M. R. Pederson, D. J. Singh, and C. Fiolhais, *ibid.* **46**, 6671 (1992).
[24] O. Jepsen and O. K. Andersen, Solid State Commun. **9**, 1763 (1971).
[25] H. J. Monkhorst and J. D. Pack, Phys. Rev. B **13**, 5188 (1976).
[26] M. Methfessel and A. T. Paxton, Phys. Rev. B **40**, 3616 (1989).
[27] P. L. Srivastava, B. C. Giessen, and N. J. Grant, Acta Metall. **16**, 1199 (1968).
[28] A. S. Mikhaylushkin, U. Häussermann, B. Johansson, and S. I.

Simak, Phys. Rev. Lett. **92**, 195501 (2004).
[29] R. W. Vaughan and H. G. Drickamer, J. Phys. Chem. Solids **26**, 1549 (1965).
[30] V. F. Degtyareva, I. K. Bdikin, and F. Porsch, J. Phys.: Condens. Matter **15**, 1635 (2003).
[31] V. F. Degtyareva, Acta Phys. Pol. A **101**, 675 (2002).
[32] A. T. Paxton, M. Methfessel, and D. G. Pettifor, Proc. R. Soc. London, Ser. A **453**, 1493 (1997).